Electronic calibration of the ATLAS LAr calorimeter

Caroline Collard[a], on behalf of the ATLAS Liquid Argon Calorimeter Group

[a] *LAL, Univ Paris-Sud, CNRS/IN2P3, Orsay, France*

Abstract

The Liquid Argon (LAr) calorimeter is a key detector component in the ATLAS experiment at the LHC, designed to provide precision measurements of electrons, photons, jets and missing transverse energy. A critical element in the precision measurement is the electronic calibration. In this article, the computation of the energy deposited in a cell is presented as well as the role of the different calibration constants, revealing the complex calibration scheme which has been put in place. Since the installation of the LAr calorimeter in the ATLAS cavern, the electronic calibration of the readout system has been continuously exercised in the commissioning phase. The large amount of collected calibration data allows careful studies of the stability of constants, like pedestals and pulse shapes. Thanks to the experience gained during the last two years, a calibration procedure has been put in place for the LHC running period.

Key words:
ATLAS, Liquid Argon calorimeter, Calibration

1. Introduction : The ATLAS LAr calorimeter

The ATLAS LAr calorimeter is a system of three sampling calorimeters with Liquid Argon (LAr) as sensitive material. Composed by 182,468 readout channels, they cover a pseudorapidity region up to $|\eta| = 4.9$.

The ElectroMagnetic (EM) Calorimeter ($|\eta| < 3.2$) is a device based on an accordion shape geometry providing an hermetic coverage in ϕ, which consists of lead absorbers and electrodes coupled to a fast electronic shaping and readout. The number of channels in the EM Calorimeter is 173,312. Two other calorimeters complete the system: the Hadronic EndCap Calorimeter (HEC) with 5632 channels in $1.5 < |\eta| < 3.2$ and the Forward Calorimeter (FCal) with 3524 cells in $3.1 < |\eta| < 4.9$. A detailed description of the detector can be found in Ref. [1, 2].

Over the η region matched to the inner detector, the fine granularity of the EM calorimeter is ideally suited for precision measurements of electrons and photons. The coarser granularity of the rest of the calorimeter is sufficient to satisfy the physics requirements for jet reconstruction and missing transverse energy measurements. The expected performances are presented in Ref. [3].

The electronic calibration plays an important role to achieve a good uniformity, and thus energy resolution over the whole calorimeter. A global constant term of 0.7 % requires that the electronic calibration contribution is below 0.25 % [4]. Calibration runs are planned to be taken beween LHC fills to provide calibration constants used online and offline for energy reconstruction.

Section 2 of this article describes the signal generation in the calorimeter up to the energy computation. The calibration procedure is presented in section 3. The strategy for LHC running period is addressed in section 4 before the concluding remarks.

2. From a particle in the calorimeter to its energy

2.1. Signal generation and readout

The LAr signal is generated by the ionization electrons drifting in the LAr gap under the high voltage between electrodes and absorbers. The peak of the ionization current is proportional to the energy released in LAr. The triangular current signal is pre-amplified and shaped (with a bipolar filter CR-RC^2), then sampled at the LHC bunch crossing frequency (every 25 ns) and digitized. In physics mode, only 5 samples are used, but it can go up to 32 for calibration and commissioning.

The ionization signal can be mimicked by a precise calibration system; the amplitude of the injected pulse is controlled by a 16bits DAC.

The dynamical range of a cell from 30 MeV to 3 TeV required by ATLAS is achieved using, on the Front End Board (FEB), amplifiers with 3 different gains in the ratio 1/10/100.

The energy is computed in the readout drivers, located in the ATLAS counting room. Other information like time and shape quality are also evaluated above a certain energy threshold. Only for a restricted number of channels (above a higher energy threshold), the 5 samples are transmitted in addition to the energy, time and quality.

Email address: collard@lal.in2p3.fr (Caroline Collard)

2.2. Energy computation

Based on the sample values s_j (in ADC counts), after pedestal (p) subtraction, the maximum amplitude of the pulse A_{max} as well as the temporal position τ is obtained by Optimal Filtering (OF) [5]:

$$A_{max} = \sum_{j=1}^{N_{samples}} a_j(s_j - p), \quad (1)$$

$$\tau = \frac{\sum_{j=1}^{N_{samples}} b_j(s_j - p)}{A_{max}}. \quad (2)$$

The a_j and b_j are the Optimal Filtering Coefficients (OFC) determined while minimizing the dispersion in A_{max} and τ arising from electronics and pile-up noise, taking into account the time autocorrelation of noise. Such a method has also the advantage for online processing of being faster than a fit. Using 5 samples, the electronic noise is reduced by a factor 1.7 with respect to a readout with only one sample. In addition to the autocorrelation matrix, the signal shape needs to be provided for every cell.

The following formula explains the needed steps to go from the amplitude A_{max} to the cell energy:

$$E_{cell} = F_{\mu A \to MeV} \cdot F_{DAC \to \mu A} \cdot \frac{1}{\frac{M_{phys}}{M_{cali}}} \cdot R \cdot A_{max} \quad (3)$$

where $F_{\mu A \to MeV}$ and $F_{DAC \to \mu A}$ are two conversion factors. The first one depends on the sampling fraction and is estimated with Geant 4 simulations and results from testbeams. The second one takes into account calibration board specificities. The R factor of eq. (3) transforms ADC into DAC values. As R is determined on calibration pulse and not directly on ionization pulse, the difference between those two pulses has to be taken into account. The calibration signal is a decreasing exponential injected at the output of the detector cell on the motherboard[1], while the ionization pulse originates from a triangular signal collected on the electrode. As a result, the shaper outputs of the ionization and calibration signal corresponding to the same initial injected current are different (see Fig. 1). The energy is corrected for the ratio of the two pulse maxima $1/(M_{phys}/M_{cali})$ in eq. (3), the ionization pulse being predicted by factorisation of the readout response [6].

All the constants of eq. (3), except the $F_{\mu A \to MeV}$ factor, are determined by calibration runs, on a cell by cell basis.

3. Description of the calibration procedure

3.1. Calibration runs

Three different types of calibration runs are taken: *pedestal*, *ramp* and *delay*.

[1]The injection resistors are mounted on the detector in the cold for the EM calorimeter and for the HEC. They are mounted on the base-plane of the front-end crates for the FCal.

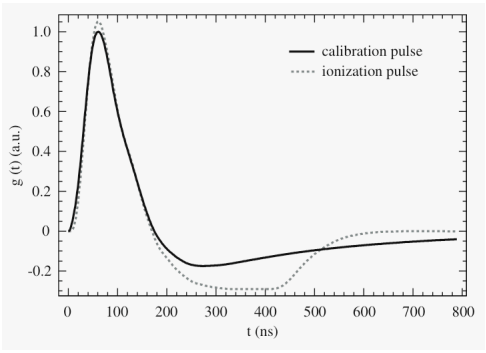

Figure 1: Typical pulse shapes from calibration signal (continuous line) and ionization signal (dotted line) in the barrel EM calorimeter.

The *pedestal* run consists of reading the detector with no input signal. It provides pedestal information from the average, noise from the RMS and noise autocorrelation from the timing correlation of the samples.

During the *ramp* run, different input current signals (DAC) are injected. The gain slope R is extracted from a fit of the DAC versus ADC curve with a first order polynomial.

For a *delay* run, one single signal amplitude is used. The calibration pulse is shifted by steps of 1.04 ns along 25 ns in order to reconstruct the pulse shape.

3.2. The chain to reconstruct calibration data

To determine the calibration constants, the following scheme has been set in place (see Fig. 2).

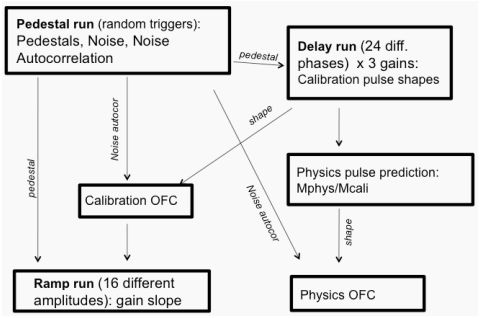

Figure 2: Block diagram of the main operations involved in the current calibration scheme.

To reconstruct the R factor coming from the *ramp* runs, one needs to know the pedestal value to be subtracted and the calibration OFC to estimate the A_{max} associated to the injected DAC signal. These calibration OFC are determined using the noise autocorrelation information from *pedestal* runs and the calibration shape from the *delay* runs (after pedestal subtraction).

To compute the physics OFC, one needs the ionization pulse shapes (whose prediction is mainly based on calibration pulses from *delay* runs) and the noise autocorrelation from *pedestal* runs. In case of high luminosity data taking, the pile-up noise autocorrelation has also to be taken

into account. This last information will be derived from minimum bias or random trigger events.

3.3. The constant stability

Frequent sets of calibration data are taken in order to test the stability of the different constants. An automatic processing has been put in place to reconstruct the data and prepare new sets of constants ready to be loaded in the ATLAS databases. The validation of those data is done with respect to a reference run. Databases are updated only if it is needed.

From recent measurements, it has been observed that in stable conditions (stable temperature, stable cooling, ...) the parameter variations are small. As shown in Fig. 3, the pedestal variation is of the order of a few MeV, which is below noise level. The relative maximum amplitude difference of the calibration pulses is at the permil level (Fig. 4). In such a case, databases do not need to be updated.

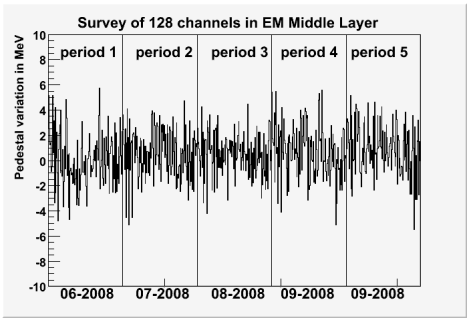

Figure 3: Pedestal variation in MeV for different time periods, for a random set (1 FEB) of channels in the EM calorimeter.

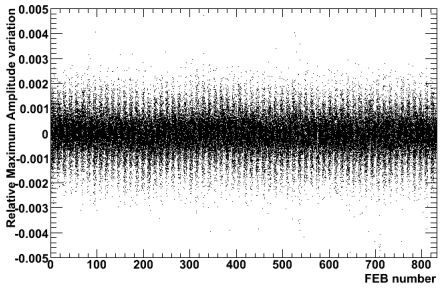

Figure 4: Relative maximum amplitude variation of the calibration pulses in the barrel EM calorimeter.

4. Strategy of calibration during LHC running

Between LHC fills ($\sim$ every 8 hours), it is planned to take *pedestal* and *ramp* runs, reconstruct them and verify the stability. In case of change, the new condition constants will be uploaded into online and offline databases. This decision has to be taken before starting the new physics runs. It has been verified that *pedestal* and *ramp* runs can be processed in less than 30 minutes. If databases are updated, in addition *delay* runs will then be taken and physics OFC will be recomputed to better understand the effect.

If everything is stable, once per week, longer calibration runs are foreseen. The stability of the calibration pulse shapes will be checked with *delay* runs (some dedicated analysis like time jitter could be added). Coherent noise could be studied with special *pedestal* runs.

In addition to calibration runs, physics runs will also be used for calibration purposes. The pedestals and noise will be monitored with random triggers. Some special data streams will be taken to monitor the real ionization pulse shapes. The pile-up and electronics autocorrelation matrix will be measured with minimum bias and/or random trigger events.

5. Conclusions

Electronic calibration is a key element to achieve a good energy resolution. A complex formula is used online (and also offline) to compute the energy deposited in the detector. The different ingredients are determined cell by cell, for the 182,468 readout channels of the LAr calorimeter, and mainly obtained from calibration runs. The extracted constants have to be monitored and updated into databases in case of change. For this purpose, a well defined strategy has been designed for the LHC running period. Since the installation of the LAr calorimeter, regular calibration runs have been taken and used successfully to commission the detector. It has been observed with the present accumulated data, that calibration constants are stable under smooth working detector conditions.

Acknowledgments

I would like to thank all the people in the ATLAS Liquid Argon Calorimeter Group involved in electronic calibration for the huge and non-sexy work that it represents. I am also grateful to those who built, integrated and installed the LAr detectors in the ATLAS cavern, and those who operate the detector on a daily basis.

References

[1] "ATLAS liquid argon calorimeter: Technical design report", ATLAS Collaboration, ATLAS-TDR-002, CERN-LHCC-96-41.
[2] "The ATLAS Experiment at the CERN Large Hadron Collider", ATLAS Collaboration, G. Aad et al., *JINST* 3 (2008) S08003.
[3] "Expected Performance of the ATLAS Experiment Detector, Trigger, Physics", ATLAS Collaboration, G. Aad et al., CERN-OPEN-2008-020 ; ISBN978-92-9083-321-5, arXiv:0901.0512.
[4] "Response uniformity of the ATLAS liquid argon electromagnetic calorimeter", M. Aharrouche et al., *NIM A*582 (2007) 429.
[5] "Signal processing consideration for liquid ionization calorimeters in a high rate environment", W.E. Cleland, E.G. Stern, *NIM A*338 (1994) 467.
[6] "Cell response equalisation of the ATLAS electromagnetic calorimeter without the direct knowledge of the ionisation signals", D. Banfi et al., *JINST* 1 (2006) P08001.